TU Delft

Delft University of Technology

Analysis and testing of a thermoplastic composite stiffened panel under compression

van Dooren, Kevin; Labans, Edgars; Tijs, Bas; Bisagni, Chiara; Waleson, J.

Publication date
2019

Document Version
Accepted author manuscript

Published in
Proceedings of 22nd International Conference on Composite Materials (ICCM22), Melbourne, AU, August 11-16, 2019

Citation (APA)
van Dooren, K., Labans, E., Tijs, B., Bisagni, C., & Waleson, J. (2019). Analysis and testing of a thermoplastic composite stiffened panel under compression. In *Proceedings of 22nd International Conference on Composite Materials (ICCM22), Melbourne, AU, August 11-16, 2019* (pp. 2336-2342). Article 5108-2

Important note
To cite this publication, please use the final published version (if applicable).
Please check the document version above.

Copyright
Other than for strictly personal use, it is not permitted to download, forward or distribute the text or part of it, without the consent of the author(s) and/or copyright holder(s), unless the work is under an open content license such as Creative Commons.

Takedown policy
Please contact us and provide details if you believe this document breaches copyrights.
We will remove access to the work immediately and investigate your claim.

This work is downloaded from Delft University of Technology.
For technical reasons the number of authors shown on this cover page is limited to a maximum of 10.

ANALYSIS AND TESTING OF A THERMOPLASTIC COMPOSITE STIFFENED PANEL UNDER COMPRESSION

Kevin S. van Dooren[1*], Edgars Labans[1], Bas H.A.H. Tijs[1,2], Jan E.A. Waleson[2] and Chiara Bisagni[1]

[1] Delft University of Technology, Faculty of Aerospace Engineering, Delft, Netherlands

[2] GKN Aerospace - Fokker, Papendrecht, Netherlands

* Corresponding author (k.s.vandooren@tudelft.nl)

Keywords: *Thermoplastic, Stiffened Panel, Buckling, Collapse*

ABSTRACT`

This paper presents the numerical analysis of a thermoplastic composite stiffened panel subjected to compression load. The panel has three stringers with a non-symmetric design, with an artificial crack at the middle stringer interface and is made from a fast crystallizing polyetherketoneketone carbon composite. The finite element model includes an approximation of the geometrical imperfections which were measured using a digital image correlation system. The finite element analyses are discussed, where the crack propagation is modelled using the virtual crack closure technique. The results show that crack propagation starts rather early after buckling and the crack growth behaviour is heavily influenced by the buckling shape, which consists of three half-waves in longitudinal direction in each bay.

1 INTRODUCTION

High performance thermoplastic materials for the use in aeronautical composite structures were introduced in the 1980's [1]. The main advantages of thermoplastic materials lay in the high toughness, chemical resistance and expanded manufacturing possibilities such as thermoplastic welding, hot press forming and co-consolidation processes [2,3]. These manufacturing techniques can result in cost reduction due to a lower number of parts to assemble and out-of-autoclave manufacturing possibilities.

In recent years several projects on thermoplastic aerostructures have been successfully executed, such as TAPAS 1 [1] and TAPAS 2 [2] in the Netherlands, or are still ongoing [4]. TAPAS 1 developed the required technology for thermoplastic primary structures and resulted in a fuselage shell demonstrator and torsion box demonstrator. TAPAS 2 developed a thermoplastic orthogrid fuselage shell with new stiffening and joining methods. The project resulted in a fuselage design without fasteners and the disposal of the "mouse hole" in the frame of the fuselage, through which the stringer normally passes. These design improvements shed two critical points of the more classical fuselage construction. The fuselage test panel that was manufactured during TAPAS 2 had an artificial crack in the stiffener joint interface, which showed no propagation during compression loading.

The further development of thermoplastic composites for primary structures is explored in the Clean Sky 2 "SmarT mUlti-fuNctioNal and INtegrated TP fuselaGe" STUNNING project, which focusses on developing a multi-functional fuselage demonstrator. Within this project, the performance of thermoplastic composite structures will be linked to the manufacturing processes, such as thermoplastic welding, and a methodology will be developed for the virtual testing of these structures.

This paper considers the analysis of a thermoplastic composite stiffened panel, with emphasis on the buckling behaviour, damage propagation and final collapse. The thermoplastic panel has three blade stringers with an angled cap on one side and was designed and manufactured by GKN Fokker. The panel includes a Barely Visible Impact Damage (BVID) at the middle stringer interface, that is modelled by the use of the Virtual Crack Closure Technique (VCCT) [5-8]. VCCT has the advantage that it shows accurate results with a relatively coarse mesh. The analysis, together with the future test of two nominal identical panels, allows to obtain a better understanding of thermoplastic structures and the effect of impact damage.

2 PANEL GEOMETRY AND MATERIAL

The three-stringer panel is shown in Figure 1. The panel is 495.3 mm long including the potting, 445.3 mm long in between the potting, and 344.8 mm in width. The web is 28 mm in height, the cap is 15 mm wide and the three stringers have a spacing of 152.4 mm. The panel has an artificial crack in the region between the filler and the skin at the middle stringer. The crack is approximately 70 mm long, as shown in the red region in Figure 1, and is considered to be BVID for this design. The artificial crack is created by a 40 mm Teflon insert, after which the crack is extended to a length of approximately 70 mm in a testing machine.

The panel is made of Fast Crystallizing PolyEtherKetoneKetone (PEKK FC) carbon unidirectional plies with additional PEKK FC glass fabric plies in the interface regions. The material properties are reported in Table 1. The additional glass fabric plies are located at the bottom of the skin, underneath the skin-stringer interface and are dropped in two steps in the transverse direction.

The cross-section of the stringer region consists of five laminated parts and the filler as shown in Figure 2. The laminated parts consist of five different layups and are joined by a short carbon fiber PEKK filler. The layups of the laminated parts and the material properties of the filler are reported in Tables 2 and 3 respectively. The laminated parts are manufactured by an automated fiber placement process, the filler material is an extrusion product, and the parts are joined by an autoclave process.

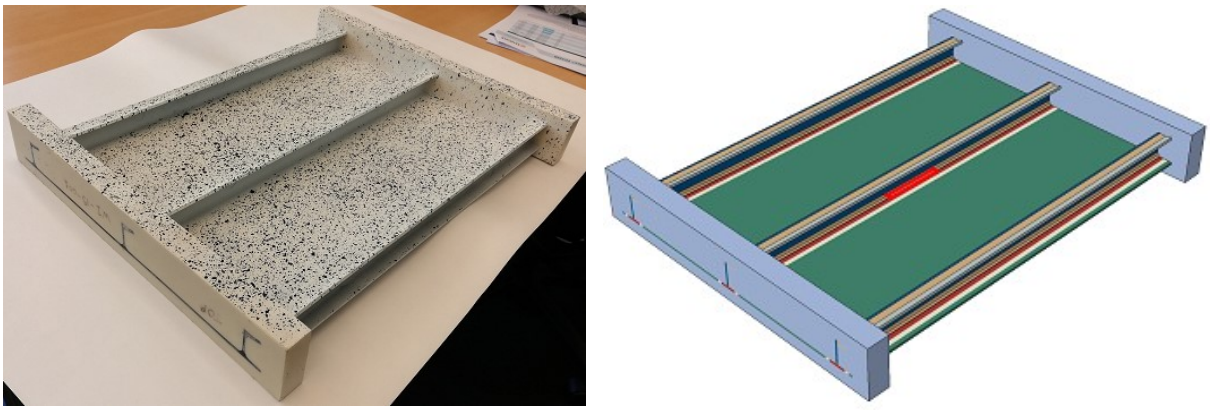

Figure 1: Three-stringer panel (left), panel geometry with artificial crack highlighted in red (right).

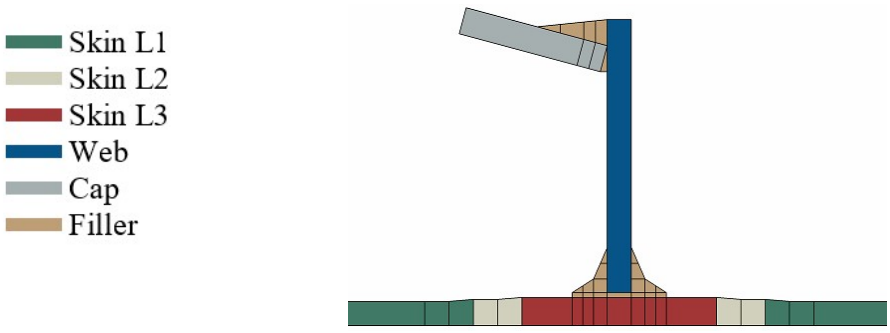

Figure 2: Stringer cross-section.

	E_{11} [MPa]	E_{22} [MPa]	ν_{12} [-]	G_{12} [MPa]	G_{13} [MPa]	G_{23} [MPa]	ρ [kg/m^3]	t_p [mm]
PEKK FC Carbon UD	126100	11200	0.3	5460	5460	3320	1560	0.138
PEKK FC Glass Fabric	25000	25000	0.3	3000	3000	2700	2200	0.1

Table 1: Material properties of PEKK FC carbon and glass plies.

Section	Thickness [mm]	Layup
Skin L1	2.484	$[45/-45/0/45/90/-45/45/0/-45]^{C}s$
Skin L2	2.684	$[0_2]^{G}$ $[45/-45/0/45/90/-45/45/0/-45]^{C}s$
Skin L3	2.848	$[0_4]^{G}$ $[45/-45/0/45/90/-45/45/0/-45]^{C}s$
Web	2.484	$[45/90/-45/0/45/0/-45/0/\underline{45/-45}]^{C}s$
Cap	2.760	$[45/90/-45/0/45/0/-45/0/0/90]^{C}s$

Table 2: Layups of three-stringer panel (C and G superscript for carbon and glass plies, respectively).

$E_{11} = E_{22}$ [MPa]	E_{33} [MPa]	$\nu_{12} = \nu_{13}$ [-]	ν_{23} [-]	$G_{12} = G_{13}$ [MPa]	G_{23} [MPa]	ρ [kg/m^3]
13252	6579	0.42	0.51	2389	2145	1560

Table 3: Material properties of PEKK short fiber carbon filler.

3 PANEL MEASUREMENTS

The geometrical imperfections of the panel were measured by the use of Digital Image Correlation (DIC). The DIC setup is shown in Figure 3. The measured imperfections can be seen in Figure 4, where they are projected onto the actual panel as a contour plot. The measurement shows a maximum out-of-plane imperfection of 0.62 mm in outwards direction, and a maximum of 1.21 mm inwards for the skin region. The panel presents a slightly V-curved shape in the transverse direction and a slight curvature in the longitudinal direction. This curvature is most likely caused by internal stresses due to the potting curing process and the mismatch in stiffness of the different materials.

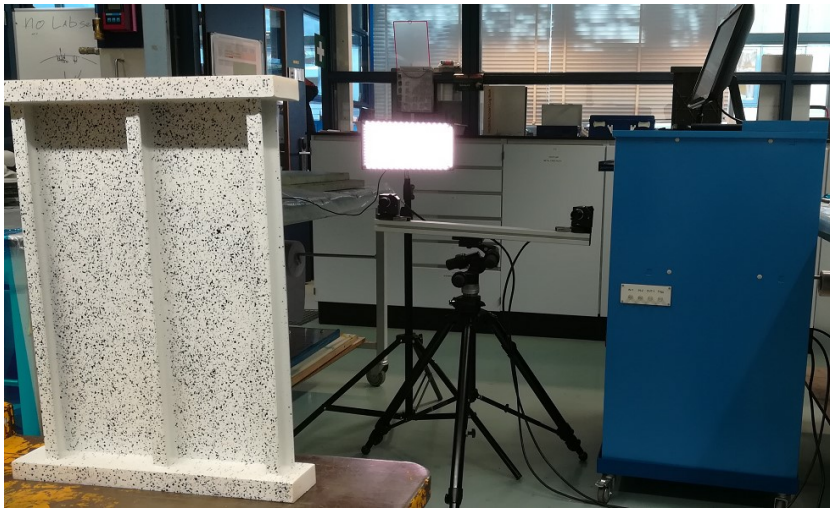

Figure 3: DIC measurement setup.

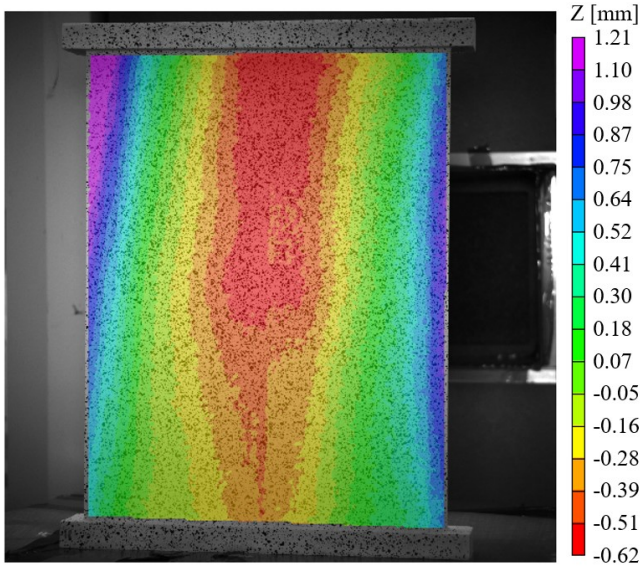

Figure 4: DIC contour plot of skin side.

4 FINITE ELEMENT ANALYSIS

The Finite Element (FE) analyses are conducted using Abaqus 2017 [9]. The general mesh size of the model is 2.5 mm and is kept as regular as possible. The laminated parts consist of continuum shell elements and the filler and potting regions consist of solid brick and wedge elements. The whole model makes use of shared nodes between different sections, except for the interface of the middle stringer between the filler and skin. This interface is partially bonded by a contact pair definition with VCCT, for which the interface properties as reported in Table 4 are used.

G_{Ic} [kJ/m^2]	G_{IIc} [kJ/m^2]	G_{IIIc} [kJ/m^2]	η [-]
1.41	1.9	1.9	2.3

Table 4: PEKK FC interface properties.

The VCCT uses a default fracture tolerance of 0.2 and an unstable crack growth tolerance of 2. This unstable crack growth option is included, as it improves convergence and computational efficiency when unstable crack growth occurs. Contact stabilisation is used to stabilise both loss of contact and separation. The damage propagation modelling methodology is verified on a Double Cantilever Beam (DCB) specimen, and validated on two single-stringer specimens which were experimentally tested by GKN Fokker. The verification and validation steps use the same meshing strategies, element types and VCCT parameters.

The imperfections as measured by DIC are approximated in the FE model of the three-stringer panel and are shown in Figure 5. The buckling load and shape of the panel are determined by a linear eigenvalue analysis, which results in a three half wave buckling anti-symmetric shape as shown in Figure 6 and a buckling load of 100 kN.

The buckling behaviour, damage propagation and final collapse of the panel are determined with a dynamic implicit analysis. The load is applied as a longitudinal displacement. The obtained load-displacement curve and crack length-displacement curve are shown in Figure 7. The panel buckles gradually at a load around 100 kN with three half-waves in the longitudinal direction, after which the stiffness of the panel is slightly reduced. Final collapse occurs at 227 kN when the panel loses its load carrying ability due to the failure of the middle stringer.

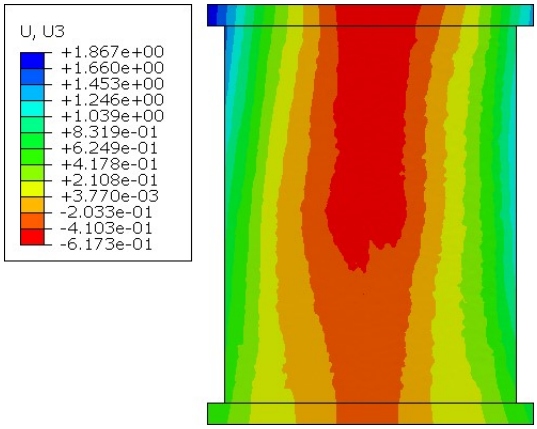

Figure 5: Imperfection approximation for finite element model in mm.

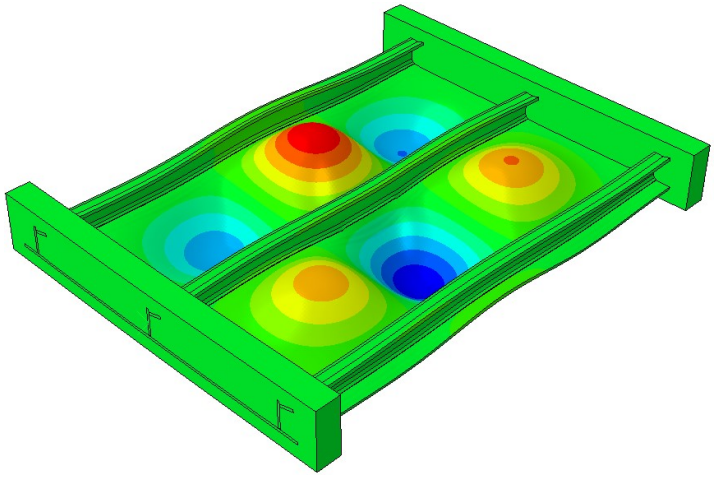

Figure 6: Buckling shape of three-stringer panel.

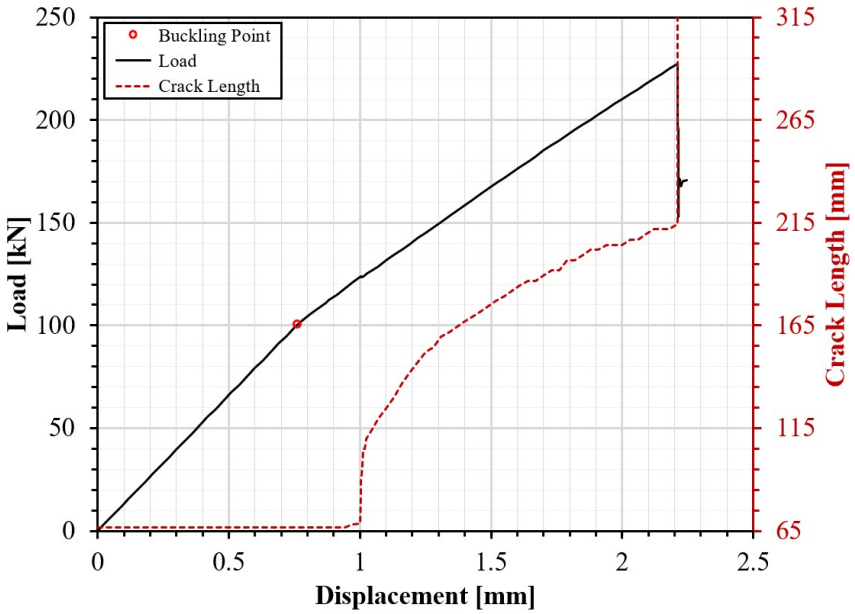

Figure 7: Numerical results for load and maximum crack length versus displacement.

Crack propagation starts at a load of 112 kN. A sudden increase in crack length is seen at a load of 124 kN which is followed by gradual crack propagation until final collapse. Final collapse can clearly be distinguished by the drop in load due to rapid crack propagation along the entire length of the panel.

The buckling shape evolution and the corresponding crack front shape are shown in Figure 8 for five load levels. The first load level corresponds to the last increment of the finite element analysis before crack propagation starts. The shapes corresponding to the second and third load level are intermediate steps between start of crack propagation and final collapse. The fourth load level is the last increment before final collapse and the fifth load level is immediately after final collapse. The crack propagates at the cap side of the stringer due to the interface at the back side of the stringer being closed by the middle inwards buckling wave. Final collapse occurs when a tunnel is formed underneath the stringer between outward buckling waves at both sides of the stringer.

The experimental test will soon be conducted to validate the finite element analyses.

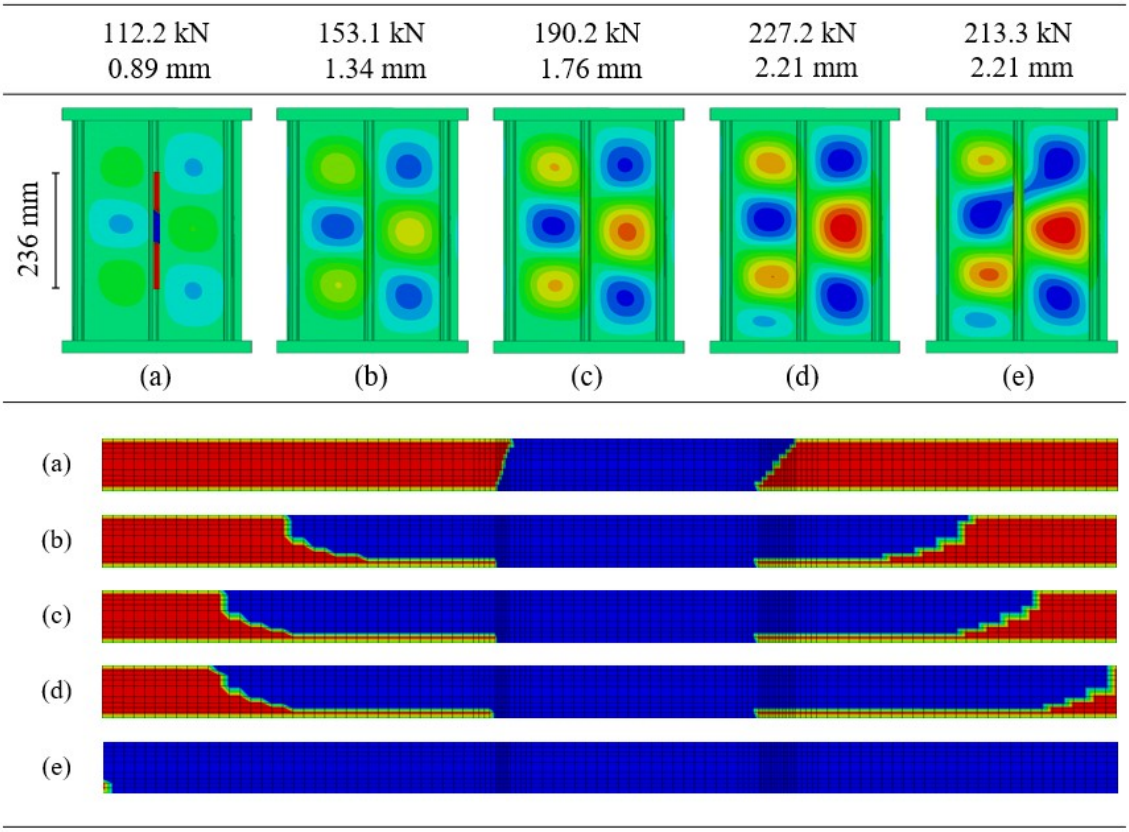

Figure 8: Evolution of post-buckling shape and corresponding crack front over a length of 236 mm.

5 CONCLUSIONS

The finite element analyses of a thermoplastic composite stiffened panel with three stringers and an artificial crack have been presented. The geometrical imperfections have been measured by digital image correlation and were approximated in the finite element model. The effect of the artificial crack on the buckling behaviour, damage propagation and final collapse was investigated. The crack opening is influenced by the non-symmetry of the stringer geometry and by the post-buckling shape. The three-stringer panel shows buckling at a load of 100 kN, which is then rather closely followed by the start of crack propagation at a load of 112 kN. The final collapse of the panel occurs at a load of 227 kN, when a tunnel forms underneath the stringer and total separation of the stringer follows.

The results of the tests of two nominally identical panels and the correlation with the finite element model will be presented at the conference.

ACKNOWLEDGEMENTS

The work presented received funding from the Clean Sky 2 Joint Undertaking under the European Union's Horizon 2020 research and innovation programme under grant agreement No 776455.

REFERENCES

[1] A. Offringa, J.W. van Ingen and A. Buitenhuis, Butt-joined, thermoplastic stiffened-skin concept development, *SAMPE Journal*, **48**, 2012, pp. 7-15.

[2] J.W. van Ingen, Thermoplastic orthogrid fuselage shell, *SAMPE Journal*, **52**, 2016, pp. 7-15.

[3] B.H.A.H. Tijs, C.S. Lopes, A. Turon, C. Bisagni, J. Waleson, J.W. van Ingen and S.L. Veldman, Virtual testing of thermoplastic composites: towards a hybrid simulation-physical testing pyramid, *ECCM18 - 18th European Conference on Composite Materials*, Athens, Greece, 2018.

[4] G. Gardiner, *Thermoplastic composite demonstrators - EU roadmap for future airframes*, Composites World, https://www.compositesworld.com/articles/thermoplastic-composite-demonstrators-eu-roadmap-for-future-airframes-.

[5] R. Krueger, An approach to assess delamination propagation simulation capabilities in commercial finite element codes, *NASA Technical Memorandum*, NASA/TM-2008-215123, 2008.

[6] R. Krueger, A summary of benchmark examples to assess the performance of quasi-static delamination propagation prediction capabilities in finite element codes, *Journal of Composite Materials*, **49**, 2014, pp. 3297-3316.

[7] C.G. Dávila and C. Bisagni, Fatigue life and damage tolerance of postbuckled composite stiffened structures with initial delamination, *Composite Structures*, **161**, 2017, pp. 73-84.

[8] C. Bisagni, P. Brambilla and C.G. Davila, Modeling delamination in postbuckled composite structures under static and fatigue loads, *SAMPE 2013 Conference and Exhibition*, 2013, pp. 1035-1049.

[9] Abaqus 2017 documentation, *Dassault Systemes Simulia Corp.*, 2017.